Available online at www.sciencedirect.com

SciVerse ScienceDirect

Physics Procedia 35 (2012) 128 – 133

Physics Procedia

Positron Studies of Defects 2011

Hydrogen-induced plastic deformation in ZnO

F. Lukáč[a]*, J. Čížek[a], M. Vlček[a], I. Procházka[a], W. Anwand[b], G. Brauer[b], F. Traeger[c], D. Rogalla[c] and H-W. Becker[c]

[a]*Charles University in Prague, Faculty of Mathematics and Physics, V Holešovičkách 2, 180 00 Praha 8, Czech Republic*
[b]*Institut für Strahlenphysik, Forschungszentrum Dresden-Rossendorf, Postfach 510119, D-01314 Dresden, Germany*
[c]*Physikalische Chemie I, Ruhr-Universitaet Bochum, Universitaetsstr. 150, D-44801 Bochum, Germany*

Abstract

In the present work hydrothermally grown ZnO single crystals covered with Pd over-layer were electrochemically loaded with hydrogen and the influence of hydrogen on ZnO microstructure was investigated by positron annihilation spectroscopy (PAS). Nuclear reaction analysis (NRA) was employed for determination of depth profile of hydrogen concentration in the sample. NRA measurements confirmed that a substantial amount of hydrogen was introduced into ZnO by electrochemical charging. The bulk hydrogen concentration in ZnO determined by NRA agrees well with the concentration estimated from the transported charge using the Faraday's law. Moreover, a subsurface region with enhanced hydrogen concentration was found in the loaded crystals. Slow positron implantation spectroscopy (SPIS) investigations of hydrogen-loaded crystal revealed enhanced concentration of defects in the subsurface region. This testifies hydrogen-induced plastic deformation of the loaded crystal. Absorbed hydrogen causes a significant lattice expansion. At low hydrogen concentrations this expansion is accommodated by elastic straining, but at higher concentrations hydrogen-induced stress exceeds the yield stress in ZnO and plastic deformation of the loaded crystal takes place. Enhanced hydrogen concentration detected in the subsurface region by NRA is, therefore, due to excess hydrogen trapped at open volume defects introduced by plastic deformation. Moreover, it was found that hydrogen-induced plastic deformation in the subsurface layer leads to typical surface modification: formation of hexagonal shape pyramids on the surface due to hydrogen-induced slip in the [0001] direction.

Keywords: zinc oxide; hydrogen; plastic deformation; nuclear reaction analysis

* Corresponding author: lukac@mbox.troja.mff.cuni.cz

1875-3892 © 2012 The Authors Published by Elsevier B.V. Selection and/or peer-review under responsibility of Organizing Committee.
doi:10.1016/j.phpro.2012.06.023

1. Introduction

Zinc oxide (ZnO) is a wide band gap semiconductor with many promising applications in optoelectronics [1]. Electrical and optical properties of ZnO crystals are strongly influenced by intrinsic point defects and their complexes with impurities. It was shown that hydrogen is the most important impurity in hydrothermally grown ZnO crystals [2]. Moreover, it was shown that a high amount of hydrogen can be introduced into ZnO crystal by electrochemical loading [3]. Understanding of hydrogen behavior in ZnO crystals is, therefore, very important. This work presents characterization of depth profile of hydrogen concentration and hydrogen-induced defects in ZnO crystal loaded with hydrogen.

2. Experimental

Hydrothermally grown ZnO (0001) single crystal (MaTecK GmbH) with dimensions 10 x 10 x 0.5 mm^3 and O-terminated surface was investigated. One face on the crystal was optically polished, while the opposite side was left unpolished. The polished surface was covered with 20 nm thick Pd over-layer deposited by cold cathode beam sputtering. The Pd over-layer is necessary for electrochemical hydrogen loading. It makes the surface electrically conductive and catalyses dissociation of H_2 molecules on the surface which facilitates hydrogen permeation into ZnO [3]. The ZnO specimens were electrochemically loaded with hydrogen in a cell filled with a 1:1 mixture of H_3PO_4 and glycerin. Hydrogen charging was performed at room temperature for 24 h by constant current of 0.3 mA using a Pt counter-electrode, while the loaded specimen was acting as cathode. The hydrogen concentration c_H introduced into the sample can be estimated from the transported charge using the Faraday's law.

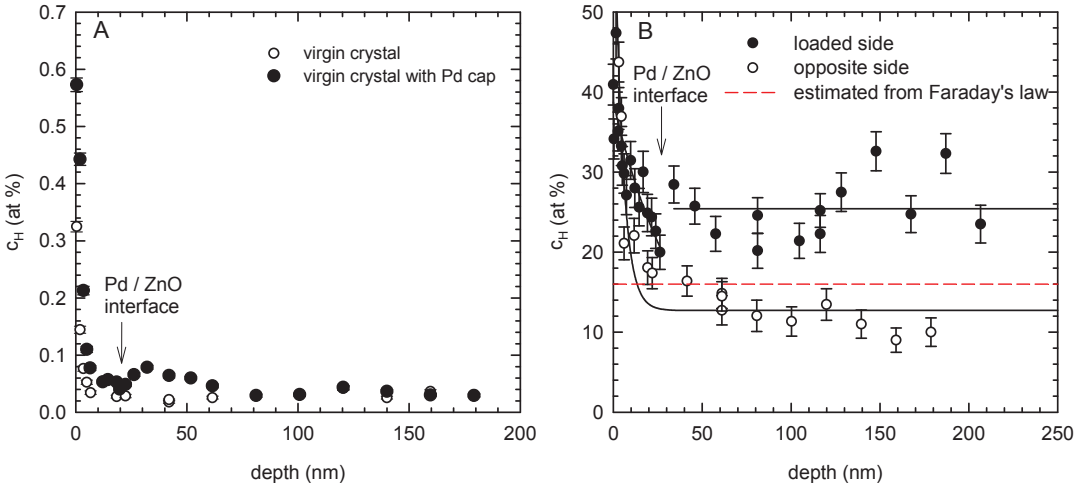

Figure 1 Depth profile of hydrogen concentration determined by NRA (A) on the virgin ZnO crystal (open points) and the virgin crystal covered with Pd cap (full points). The position of the Pd/ZnO interface is indicated by arrow; (B) on the ZnO crystal loaded with hydrogen. NRA investigations were performed on the loaded side covered with Pd cap (full points) and on the opposite side (open points). Solid lines show fit by exponentially decaying function, dashed line indicates hydrogen concentration estimated from the transported charge using the Faraday's law.

The hydrogen concentration introduced into the sample was determined by NRA using the nuclear reaction $^{15}N + {}^{1}H \rightarrow {}^{12}C + {}^{4}He + \gamma$–rays [4]. Energy of bombarding ^{15}N ions was gradually increased

from 6.39 to 7.1 MeV. This corresponds to the penetration depth into ZnO from the surface up to 260 nm.

Positron lifetime (LT) measurements were performed with a 1.5 MBq $^{22}Na_2CO_3$ positron source deposited on a 2 μm thick mylar foil and sandwiched between a pair of ZnO crystals. A digital LT spectrometer [5] with excellent time resolution of 145 ps (FWHM ^{22}Na) was employed for LT investigations. At least 10^7 positron annihilation events were accumulated in LT spectra which were decomposed using a maximum likelihood based procedure [6]. The source contribution consisted of two weak components with lifetimes of ~368 ps and ~1.5 ns and intensities of ~7 % and ~1 %, respectively.

SPIS investigations were carried on a magnetically guided variable energy slow positron beam SPONSOR [7]. Energy of incident positrons was varied in the range from 0.03 to 36 keV. Doppler broadening of annihilation profile was measured by HPGe detector with energy resolution of 1.09 ± 0.01 keV (FWHM) at 511 keV and analyzed using *S* and *W* line shape parameters. All *S* parameters presented in this work were normalized to the bulk value S_0 = 0.5068(5) measured on the virgin ZnO crystal at positron energy of 36 keV. Similarly *W* parameters were normalized to the bulk value W_0 = 0.1039(7). Dependence of the *S* parameter on positron energy was fitted using the VEPFIT software package [8].

Table 1 Results of PAS and NRA investigations of ZnO crystals: positron lifetime τ_D determined by LT spectroscopy; bulk hydrogen concentration c_H determined by NRA; hydrogen concentration estimated from the transported charge using the Faraday's law; concentration of open-volume defects c_D obtained from SPIS measurements using Eq. (2).

State of ZnO crystal	τ_D (ps)	c_H (at.%) measured by NRA	c_H (at.%) Faraday's law	c_D (ppm)
virgin-polished side	181.9(3)	0.03(1)	-	37(6)
virgin-unpolished side	181.6(3)	not analyzed	-	37(6)
virgin+Pd cap	182.0(2)	0.03(1)	-	52(9)
H-loaded 3 h (loaded side)	179.6(2)	4.0(5)	4.2	not analyzed
H-loaded 24 h (loaded side)	178.8(4)	25(1)	16.0	76(7)
H-loaded 24 h (opposite side)	178.9(3)	13(1)	16.0	66(6)

3. Results and discussion

Fig. 1(A) shows the depth profile of hydrogen concentration c_H in the virgin ZnO crystal. A sharp increase of hydrogen concentration on the surface is due to weakly bound adsorbed hydrogen molecules. The bulk hydrogen concentration in the virgin crystal is $c_H \approx 0.03$ at.%. No increase in the bulk hydrogen concentration was found after deposition of Pd cap. However, there is a hump on the hydrogen c_H profile at the Pd/ZnO interface due to excess hydrogen trapped at open-volume misfit defects at the interface.

Results of LT investigations are shown in Table 1. The virgin ZnO crystal exhibits a single component spectrum with lifetime of $\tau_D \approx 182$ ps both on the polished and the unpolished side. This is in agreement with results published in Ref. [2] and can be attributed to positrons trapped at Zn-vacancies associated with hydrogen (V_{Zn} + H). Virtually the same results were obtained after deposition of Pd cap.

Fig. 2 shows the dependence of the *S* parameter on the energy *E* of incident positrons. At very low energies virtually all positrons annihilate on the surface. With increasing energy positrons penetrate deeper and deeper into the crystal and the fraction of positrons diffusing back to the surface decreases which is reflected by a decrease of the *S* parameter from the surface value to the bulk value corresponding to the situation when all positrons annihilate in ZnO bulk. The *S(E)* curve measured on the virgin crystal was fitted by a model curve calculated by VEPFIT [8] assuming a homogeneous single layer. The results of fitting are listed in Table 2. The positron diffusion length in the virgin ZnO crystal L_+ = (58 ± 2) nm obtained from fitting is significantly shorter than positron diffusion lengths in a perfect (defect-free) semiconductors [9]. This testifies that the virgin crystal contains a significant concentration of positron

traps. This result is in concordance with LT investigations which showed saturated positron trapping in V_{Zn}+H complexes. The concentration c_D of positron traps can be calculated from the expression

$$c_D = \frac{1}{\nu_D \tau_B}\left(\frac{L_{+,B}^2}{L_+^2} - 1\right), \quad (1)$$

where τ_B = 154 ps is the bulk ZnO positron lifetime [3], ν_D is the specific positron trapping rate to V_{Zn}+H complexes and $L_{+,B}$ is the positron diffusion length in a perfect (defect-free) ZnO crystal. The concentration of V_{Zn}+H complexes obtained from Eq. (1) assuming $\nu_D = 1 \times 10^{15}$ s^{-1} which is a typical value for neutral vacancies in semiconductors and $L_{+,B}$ = 150 nm [9] is given in Table 1.
If the free positron component can be resolved in LT spectrum the concentration of positron traps can be calculated using the two state trapping model

$$c_D = \frac{1}{\nu_D}\frac{I_2}{I_1}\left(\frac{1}{\tau_B} - \frac{1}{\tau_D}\right), \quad (2)$$

where I_1 and I_2 are relative intensities of the free positron component and the contribution of positrons trapped at defects, respectively. From Eq. (2) it follows that the concentration of V_{Zn}+H complexes $c_D \approx 3.7 \times 10^{-5}$ determined in the virgin crystal by SPIS corresponds to the intensity of the free positron component $I_1 \approx 3\%$. Since it is extremely difficult to resolve the free positron component when I_1 falls below 5 %, the defect density in the virgin crystals is so high that it leads to a single component LT spectrum due to saturated positron trapping. Deposition of Pd cap modifies the *S(E)* curve in the low energy region due to positrons annihilated in the Pd over-layer. However at higher energies the *S(E)* curve remains virtually the same testifying that deposition of Pd did introduce additional defects into the crystal.

Fig. 1(B) shows depth profile of hydrogen concentration in the loaded crystal. NRA measurements were performed both on the loaded side (covered with Pd cap) and also on the opposite (unpolished) side. It is clear from the figure that hydrogen concentration in the loaded crystals is substantially higher than in the virgin sample. Moreover, NRA investigations revealed that hydrogen concentration on the loaded side is higher than on the opposite side. Detailed NRA investigations performed in Ref. [10] on a ZnO crystal loaded for a shorter time (3 h) revealed that bulk hydrogen concentration in the loaded crystal is in reasonable agreement with the value estimated from the Faraday's law. However a subsurface region with enhanced hydrogen concentration is formed on the loaded side. With increasing loading time the hydrogen-enhanced region extends deeper into the crystal. From NRA results in Fig. 1(B) we can conclude that in the crystal loaded for 24 h the thickness of hydrogen enhanced subsurface layer is higher than 250 nm. Formation of subsurface region with enhanced hydrogen concentration can be explained by excess hydrogen atoms trapped at open volume defects introduced by hydrogen-induced plastic deformation. It is well known [11] that absorbed hydrogen causes significant expansion of ZnO lattice. At very low hydrogen concentrations this expansion is accommodated by elastic strain, but from certain critical hydrogen concentration hydrogen-induced stress exceeds the yield stress in ZnO and plastic deformation takes place. It should be mentioned that interesting surface modification consisting of hexagonally shaped pyramids was observed on the surface of hydrogen loaded ZnO crystals [3]. These pyramids were most probably formed by hydrogen-induced slip in the [0001] direction.

Fig. 2 shows that hydrogen loading leads to a large increase of *S* parameter in a subsurface region corresponding to the positron energy range 1-14 keV. Hence, SPIS results testify that a subsurface region with very high concentration of defects was formed by hydrogen loading due to hydrogen-induced plastic deformation. The subsurface region with high density of defects was found both on the loaded side and the opposite side. As shown schematically in Fig. 2 the *S(E)* curves of hydrogen loaded crystals were fitted by a model consisting (i) Pd cap (on the loaded side only), (ii) subsurface layer with very high

concentration of defects and (iii) bulk ZnO layer. Results of fitting are shown in Table 2. On the loaded side the subsurface region is thicker and contains higher density of defects which is reflected by higher *S* parameter. Since the thickness of the hydrogen-enriched defected layer is higher than maximum penetration depth of ^{15}N ions, NRA probes exclusively the defected subsurface layer. Higher hydrogen concentration detected on the loaded side by NRA is in concordance with higher defect density determined on the loaded side by SPIS. The hydrogen-loaded sample exhibits enhanced *S*-parameter also in the layer (iii). Hence, the region affected by hydrogen-induced plastic deformation extends to depth of at least 2 μm corresponding to the mean penetration depth of positrons with energy E = 35 keV. However the concentration of hydrogen-induced defects rapidly diminishes with depth since the bulk Doppler broadening measurements with fast positrons from ^{22}Na source (the mean penetration depth ~ 50 μm) did not reveal any significant change of S parameter in the hydrogen-loaded crystal.

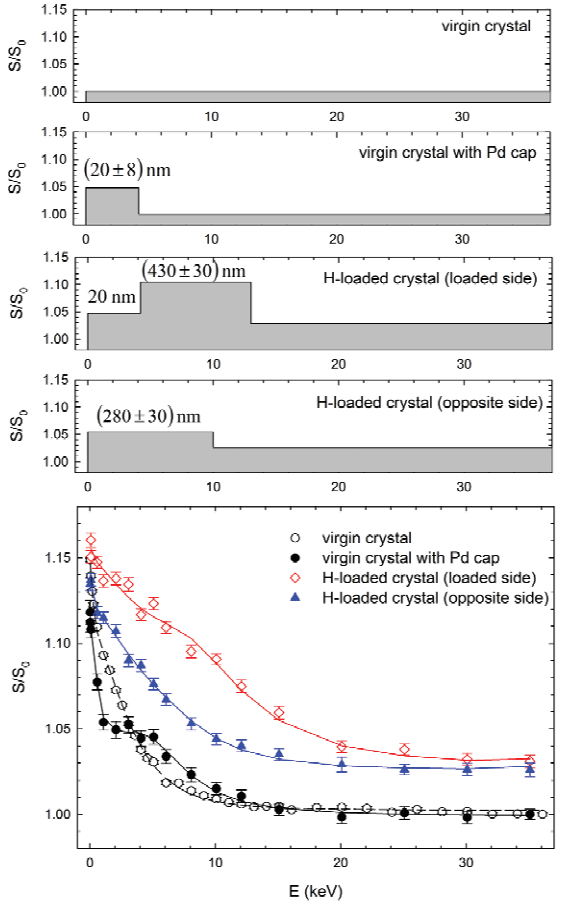

Figure 2 Dependence of the *S* parameter on positron energy *E* for the virgin crystal, the virgin crystal covered with Pd cap, and the hydrogen loaded crystal. Solid lines show fits performed using layer models shown in the upper panels. A single layer model was assumed for the virgin crystal, two layer model consisting of Pd cap and ZnO bulk was used for the virgin crystal covered with Pd cap. The *S(E)* curve of hydrogen-loaded crystal was fitted using three layer model consisting of Pd cap, defect-rich subsurface layer and ZnO bulk, while the *S(E)* curve measured on the opposite side consisted of two layers: defect-rich subsurface layer and ZnO bulk. Thicknesses of the layers obtained from fitting are shown in the upper panels. To reduce number of free parameters in fitting of hydrogen-loaded crystal (loaded side) the thickness of Pd cap was fixed at 20 nm determined previously on the virgin crystal.

Table 2 Results of fitting of *S(E)* curves by VEPFIT [8]. Layer models used in fitting of various samples are shown in Fig. 2. Each layer (i = 1,2,3) is characterized by S-parameter S_i, positron diffusion length L_{i+} and thickness t_i. The following layers were assumed in fitting: Pd cap (i=1), subsurface layer with high density of defects introduced by H-induced plastic deformation (i=2) and ZnO bulk (i=3, infinite thickness assumed). Note that positron diffusion length L_{1+} and thickness t_1 of Pd cap were fixed in fitting of *S(E)* curve of H-loaded crystal (measured from loaded side) to reduce the number of free parameters.

State of ZnO crystal	Surface	Pd cap			Defected subsurface layer			ZnO bulk	
	S_{surf}	S_1	L_{1+} (nm)	t_1 (nm)	S_2	L_{2+} (nm)	t_2 (nm)	S_3	L_{3+} (nm)
virgin	1.15(1)	-	-	-	-	-	-	1.0000	58(2)
virgin+Pd cap	1.12(1)	1.05(1)	10(5)	20(8)	-	-	-	1.004(4)	50(10)
H-loaded (loaded side)	1.167(4)	1.05(1)	10 Fix	20 Fix	1.104(4)	20(5)	430(30)	1.028(3)	42(5)
H-loaded (opposite side)	1.140(4)	-	-		1.055(8)	30(8)	280(30)	1.026(5)	45(5)

4. Conclusions

NRA investigations performed in this work confirmed that hydrogen is introduced into ZnO crystals by electrochemical charging and revealed enhanced hydrogen concentration in the subsurface region. SPIS studies revealed that hydrogen loading leads to formation of a subsurface layer with very density of defects. This can be explained by hydrogen-induced plastic deformation which introduces open volume defects acting as trapping sites for hydrogen. Enhanced hydrogen concentration in the subsurface region is due to excess hydrogen atoms trapped at open volume defect introduced by plastic deformation.

Acknowledgements

This work was supported by the Czech Science Foundation (project P108/11/0958), the Ministry of Schools, Youths and Sports of the Czech Republic (project 0021620834) and grant SVV-2010-261303.

References

[1] Ü. Özgür, Ya. I. Alivov, C. Liu, A. Teke, M. A. Reshchikov, S. Dogan, V. Avrutin, S.-J. Cho, and H. Morkoc, J. Appl. Phys. 98 (2005), 041301.

[2] G. Brauer, W. Anwand, D. Grambole, J. Genzer, W. Skorupa, J. Čížek, J. Kuriplach, I. Procházka, C.C. Ling, C.K. So, D. Schultz and D. Klimm, Phys. Rev. B 79 (2009), 115212.

[3] J. Čížek, N. Žaludová, M. Vlach, S. Daniš, J. Kuriplach, I. Procházka, G. Brauer, W. Anwand, D. Grambole, W. Skorupa, R. Gemma, R. Kirchheim and A. Pundt, J. Appl. Phys. 103 (2008) 053508

[4] W.A. Lanford, in: Handbook of Modern Ion Beam Materials Analysis, edited by R. Tesmer and M. Nastasi, Materials Research Society, Pittsburg (1995) p. 193

[5] F. Bečvář, J. Čížek, I. Procházka, J. Janotová, J. Nucl Instrum Methods A 539 (2005) 372.

[6] I. Procházka, I. Novotný, F. Bečvář, Mater. Sci. Forum 255-257 (1997) 772.

[7] W. Anwand, H.-R. Kissener, and G. Brauer, Acta Phys. Pol. A 88 (1995) 7.

[8] A. van Veen, H. Schut, M. Clement, J. de Nijs, A. Kruseman, M. IJpma: Appl. Surf. Sci. 85 (1995) 216.

[9] R. Krause-Rehberg, H.S. Leipner, Positron Annihilation in Semiconductors – Defect Studies (Springer, Berlin 1999).

[10] J. Čížek, F. Lukáč, M. Vlček, I. Procházka, F. Traeger, D. Rogalla, H.-W. Becker, Defect Diffusion Forum (2011) in print.

[11] C. G. Van de Walle, Phys. Rev. Lett. 85 (2000) 1012 33.